

Research article

Beyond Boundaries: User-Centered Product Design and Validation of a Mechanical Female Left Arm Low-Elbow Prosthesis for CrossFit Training

Edgar Isaac Rivas Hernández^{1*} and Oscar Farrerons Vidal²

¹ Department of Graphic Engineering and Design, Escola Tècnica Superior d'Enginyeria Industrial de Barcelona (ETSEIB), Universitat Politècnica de Catalunya, Av. Diagonal, 647. 08028, Barcelona (Spain)

² Department of Graphic Engineering and Design, Escola d'Enginyeria de Barcelona Est (EEBE), Universitat Politècnica de Catalunya, Av. d'Eduard Maristany, 16, Edificio A, 08019, Barcelona (Spain)

Received: March 4, 2024 | Accepted: May 24, 2025 | Published: June 29, 2025

* e-mail: edgar.isaac.rivas@upc.edu; ORCID: 0009-0002-3588-7222

DOI: 10.24310/p56-idj.5.1.2025.19239

Abstract

The objective of this work was to design and preliminarily validate a mechanical prosthesis for a female patient with below-elbow agenesis, emphasizing a user-centered product design approach. The device is intended to assist in CrossFit training, enabling dynamic movement while improving muscular balance and quality of life. The project involved the design of the forearm structure using polymer matrix composite material (epoxy resin) reinforced with laminated carbon fiber (prepreg), excluding the hand and wrist mechanisms from the current scope.

SolidWorks software was employed for mechanical design and simplified validation, while composite material properties were estimated through the micromechanical Chamis model using eLamX software. Despite the innovative integration of CAD tools, important simplifications were necessary, particularly regarding dynamic loading assumptions and socket coupling, which are acknowledged as limitations.

This work demonstrates the potential of multidisciplinary collaboration in prosthetic development, although further research and testing are required before manufacturing a fully operational device. Ethical approval was obtained from the relevant institutional review board, and the patient's informed consent was secured in accordance with the Declaration of Helsinki.

Key words: Simulation, Product design; Prototype; Product development; Case Study; Social innovation; Customization

Introduction

Left arm agenesis represents a rare congenital anomaly occurring during embryonic development. This condition

results in a unilateral or bilateral disruption of either the proximal or distal growth of the upper limbs (Dohin et al., 2016). Consequently, individuals affected by this congenital defect exhibit either complete or

partial absence of the left upper limb from birth. Clinically, this condition commonly presents as a transverse defect resembling a transradial amputation (below the elbow, as depicted in Figure 1), characterized by adequate soft tissue coverage of the distal portion and the presence of knuckles or nodules, referred to as *mamelons*.

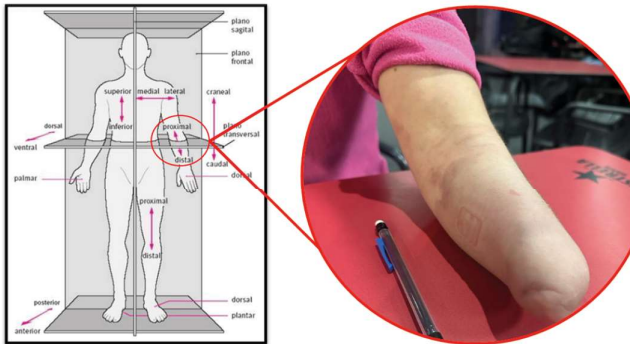


Figure 1. Transverse defect, transradial amputation type [Own source]

This congenital abnormality can result from genetic factors, environmental influences, or a combination of both (Dolk et al., 2010). The impact of agenesis on an individual's life can vary significantly, often presenting challenges related to functionality, mobility, and muscular imbalances within the body. Agenesis affects not only physical functionality but also significantly impacts mobility, muscular balance, and the psychological well-being of patients (Dolk et al., 2010). A personalized prosthetic device can greatly enhance users' independence, self-esteem, and participation in demanding physical activities.

Beyond individual cases, upper limb absence affects a substantial portion of the population. According to the World Health Organization, approximately one million limb amputations are performed globally each year, with projections suggesting that this number will increase due to trauma, vascular diseases, and congenital conditions. In Spain, approximately 60,000 individuals are living with some form of amputation (Valero, 2023). However, access to functional prostheses, particularly for sports and active lifestyles, remains extremely limited due to prohibitive costs and low availability in public healthcare systems.

According to the World Health Organization (WHO), access to assistive technologies, such as prosthetic and orthotic devices, remains critically limited worldwide, with only one in ten individuals who require these products receiving them. This significant gap in access is primarily attributed to several interrelated barriers, including the high financial cost of such devices, limited public awareness of their availability and benefits, and a widespread shortage of adequately trained professionals and specialized healthcare services (World Health Organization, 2017). This inequitable distribution of assistive products not only undermines the functional autonomy and mobility of individuals but also generates far-reaching consequences by restricting their opportunities for meaningful social inclusion, active participation in community life, and access to economic activities.

The price of advanced myoelectric prostheses can exceed €40,000, excluding most patients from access to such devices (Belter et al., 2013). Standard prostheses are typically designed for everyday use and cannot withstand the high-intensity, repetitive movements in sports like CrossFit. This creates a clear need for prosthetic solutions that balance mechanical robustness, cost-efficiency, and athletic usability.

Mari Carmen, a 34-year-old woman born with left forearm agenesis, seeks to improve her athletic performance in CrossFit —a sport characterized by dynamic, high-intensity functional movements. This real-world case underscores the urgent need for prosthetic solutions designed from a user-centred perspective, ensuring alignment between the functional goals of the patient and the mechanical performance of the device.

From a product design perspective, such needs call for approaches that go beyond traditional biomechanical engineering and consider human-based design methodologies, engaging patients in the development, iteration, and validation of prosthetic components (Cordella et al., 2016). The active involvement of the user

ensures that the prosthesis accommodates their daily and sporting habits, muscular asymmetries, and comfort expectations, thus improving long term adoption and physical performance.

Incorporating sustainable materials and manufacturing processes into prosthetic design aligns with global efforts to achieve the United Nations Sustainable Development Goals (SDGs), particularly SDG 3 (Good Health and Well-being) and SDG 12 (Responsible Consumption and Production). The use of biodegradable materials, such as polylactic acid (PLA), and recycled components can reduce environmental impact and promote a circular economy in prosthetics manufacturing in daily activities usages (Orthotic & Prosthetic Centers, 2023).

Furthermore, advancements in 3D printing technology have enabled the production of customized prosthetic limbs that are both cost-effective and environmentally friendly. By utilizing sustainable materials and additive manufacturing techniques, it is possible to create prostheses that meet individual needs while minimizing waste and resource consumption (The Guardian, 2017).

The main objective of this work is to design and preliminarily validate the forearm structure of a mechanical prosthesis to support CrossFit training, using composite materials and commercial CAD tools. This initial development phase explicitly excludes the design of the hand and wrist (socket) mechanisms, which will be addressed in future work.

The scope of the study is limited by necessary modeling and simulation simplifications, particularly in dynamic loading conditions and socket connection issues. These constraints are acknowledged throughout the document to ensure methodological transparency.

Methodology

Physical acquisition of design parameters:

Before initiating the digital modeling process, physical measurements were conducted on both arms of the patient. On the right arm, three radial reference marks were placed distally: one at 40 mm from the condyle, and two additional marks at 100 mm intervals along the forearm (Figure 2.a). The total distance from the condyle to the ulna's head was recorded as 240 mm. A similar procedure was followed for the left residual limb ("stump"), where two marks were placed at 40 mm and 100 mm from the condyle (Figure 2.b), with a total length of 170 mm.

Circumferential measurements at each mark were performed to estimate corresponding diameters of right arm (d_e , d_i , d_f) and left arm (d_i , d_e), as illustrated in Figure 3 and summarized in Table 1. These geometric parameters, directly obtained from the patient, were cross validated with 3D scan outputs to ensure consistency, reducing measurement error to within $\pm 3\%$ across key dimensions.

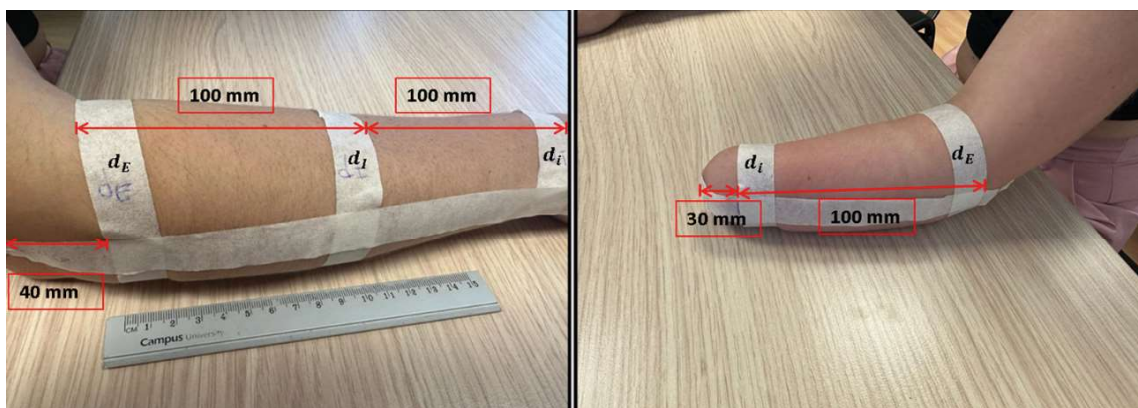


Figure 2. Placement of reference marks on a) the right arm b) the left arm [Own source]



Figure 3. Measurement of reference circles on a) the right arm b) the left arm [Own source]
amputation type [Own source]

Table 1. Summary of calculations and measurements of design parameters [Own source].

		RIGHT ARM			LEFT ARM		
		d_E	d_I	d_i	d_E		d_i
FORMULAS		RESULTS (mm)					
Perimeter	$P = 2\pi r$	240	208	149	214		140
Radius	$r = \frac{P}{2\pi}$	38,2	33,1	23,7	34,1		22,3
Diameter	$d = 2r$	76	66	47	68		44
		Condyle-wrist length (mm)			Condyle-stump length (mm)		
		240			170		

Digital acquisition of design parameters:

In addition to manual measurements, a 3D scan using Polycam LiDAR technology was conducted to capture the morphology of both arms. While 3D scanning ensures greater spatial resolution, the complementary use of 2D measurement was justified for critical dimensions such as reference diameters, given the potential noise and irregularities in point cloud data (especially at edges and occluded zones). This hybrid acquisition approach balanced accuracy and data processing efficiency. Figure 4 shows the raw scan results and the processing steps taken to delimit the working volume before importing the mesh into SolidWorks.

Prior to embarking on the modeling process for the prosthetic components, it was crucial to calibrate the scale of the digital format to correspond with real dimensions. Utilizing the compiled dataset, as outlined in Table 1, the Condyle-Wrist Length was determined, establishing the distance between d_E and d_i at 200 mm.

Subsequently, utilizing the measurement tool within SolidWorks on the data mesh, a measurement of 0.1998 mm was obtained between identified points d_E , and d_i . A scaling factor of 1000% was applied to match the real anatomical distance of 199.8 mm as shown in Figure 5.

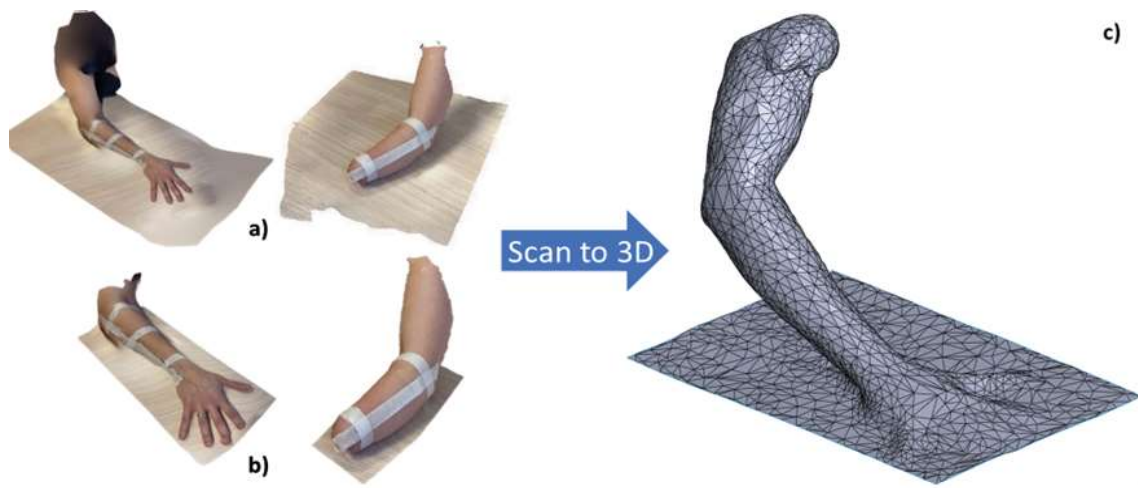


Figure 4. a) Scanning result of both extremities. b) Result of the maximum delimitation of the working volume. c) Imported data into SolidWorks after pre-processing treatment. [Own source].

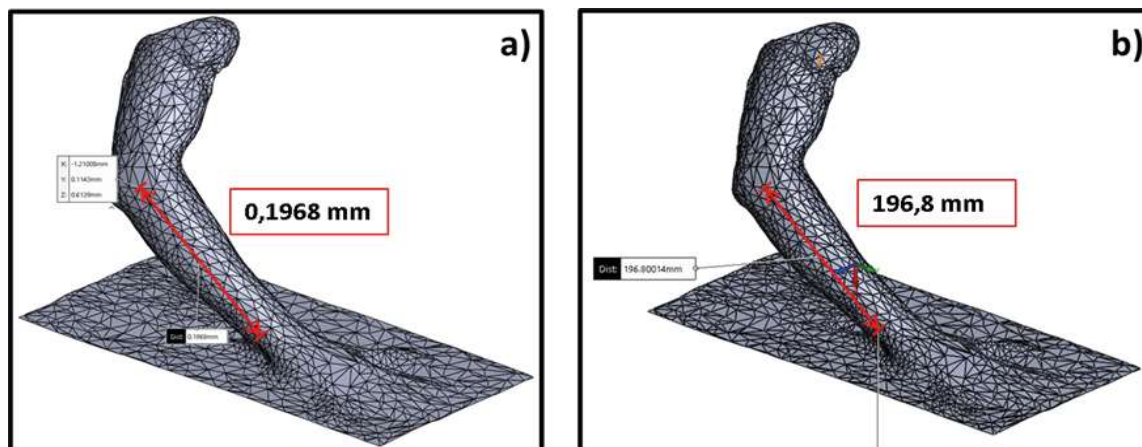


Figure 5. a) Reference distance before scaling adjustment, b) Reference distance after a 1000% scale adjustment [Own source].

Mechanical design:

Specifications regarding the mechanical stress characteristics for the forearm were established. Given the novel and pioneering nature of this project, there are no existing precedents or available data in scientific or sports literature concerning the levels and types of stress to which a prosthesis intended for CrossFit exercises may be subjected. Therefore, for this design stage, the geometric parameters obtained from the patient were coupled with the following mechanical parameters. These parameters represent a collaborative estimation by Mari Carmen, based on her sports objectives and training frequency.

For design and simulation in SolidWorks, several assumptions and simplifications were made regarding the workload on the prosthesis.

To assess the response of the prosthesis during pull-up exercises, it was assumed

that the component would undergo pure tension, considering a maximum patient weight of 90 kg.

$$\text{Traction Force: } \left[\left(\frac{90 \text{ kg}}{2} \right) * 9.81 \text{ m/s} \right] = 340 \text{ N.}$$

When evaluating the performance of the prosthesis during devil press, push-ups, military press, and handstand exercises, it is assumed that the component will undergo pure compression. This entails a maximum weight handling capacity of 35 kg per arm.

$$\text{Compression Force: } \left[\left(\frac{90 \text{ kg}}{2} \right) * 9.81 \text{ m/s} \right] = 440 \text{ N.}$$

Other exercises (bicep curls, kettlebell swings) were acknowledged to involve combined torsion and bending loads but were excluded at this stage.

While it is recognized that dynamic movements such as pull-ups and push-ups involve complex, time-varying loads, these simplifications were necessary to

enable preliminary static validation within SolidWorks. Further dynamic simulation studies are recommended for future phases to ensure safety under real CrossFit conditions.

Estimation of the mechanical properties of the laminae by means of eLamX:

The mechanical properties of a lamina of epoxy resin polymer matrix composite material reinforced with long carbon fibers were derived from the individual characteristics of each constituent component using eLamX free software from Dresden University, based on the Chamis Model, also known as the “Modified Law of Mixtures”. The individual elastic properties of the commercial reference XC 130 300g UD Prepreg Carbon Fiber, manufactured by Easy Composites, are summarized in Table 2 as input parameters.

Table 2. Summary of matrix and reinforcement properties [Own with data from Ali &

Epoxy Matrix Data:			T700 carbon fiber reinforcement data		
$\rho_m =$	1,2	g/cm^3	$\rho_f =$	1,8	g/cm^3
$E_m =$	3500	MPa	$E_{\parallel f} =$	379212	MPa
$G_m =$	1296,2962	MPa	$E_{\perp f} =$	62053	MPa
$\nu_m =$	0,35		$G_{\parallel f} =$	75842	MPa
$X_{tm} =$	55	MPa	$G_{\perp f} =$	48263	MPa
$X_{cm} =$	103	MPa	$\nu_{Lrf} =$	0,2	
$S_m =$	55	MPa	$\nu_{rrf} =$	0,25	
$\nu_f =$	0,6		$X_{tf} =$	2500	MPa
			$X_{cf} =$	1500	MPa

Within the eLamX interface, the material XC 130 300g UD is generated, incorporating the properties outlined in Table 2. The volume percentage of fibers is set at 60%, and the micromechanical Model of Chamis is selected to estimate the combined properties. As a result, eLamX outputs provided elastic constants (E_1 , E_2 , G_{12} , ν_{12}), which were then imported manually into SolidWorks to define a custom orthotropic material (“XC130 300g UD Prepreg Carbon Fibre”) for simulations. This establishes the workflow integration between eLamX and SolidWorks. The combined mechanical properties of the composite sheet are displayed in Table 3 as design parameters.

Table 3. Summary of the estimation of the elastic and resistant properties of the laminae [Own source].

CHAMIS MICROMECHANICAL MODEL					
$\rho =$	1,56	g/cm^3	$G_{xy} =$	5.432	MPa
$E_x =$	228.927	MPa	$G_{xz} =$	5.432	MPa
$E_y =$	13.007	MPa	$G_{yz} =$	5.265	MPa
$E_z =$	13.007	MPa	$X_t =$	1.500	MPa
$\nu_{xy} =$	0,26		$Y_t =$	46	MPa
$\nu_{xz} =$	0,26		$X_c =$	900	MPa
$\nu_{yz} =$	0,2352		$Y_c =$	86	MPa
$SC =$	46	MPa	$L_e =$	1.350	MPa

The accuracy of the micromechanical estimations was cross validated by comparing graphic (“carpet plot”) predictions with Classical Lamination Theory (CLT) results, showing deviations below 4%, which is considered acceptable for preliminary mechanical design stages.

Furthermore, a quasi-isotropic laminate stacking sequence $[0^\circ/45^\circ/-45^\circ/90^\circ]_s$ was selected to approximate isotropic in-plane behavior, ensuring uniform mechanical response under multidirectional loads.

Graphic estimation of the “quasi-isotropic” of the laminate:

The “quasi-isotropic” point in a laminate set is identified as the stacking sequence that approaches isotropic behavior within the plane. This entails achieving a mechanical response that is uniform in all directions. This is typically accomplished through the selection of a symmetric and balanced stacking sequence. The objective is to evenly distribute the

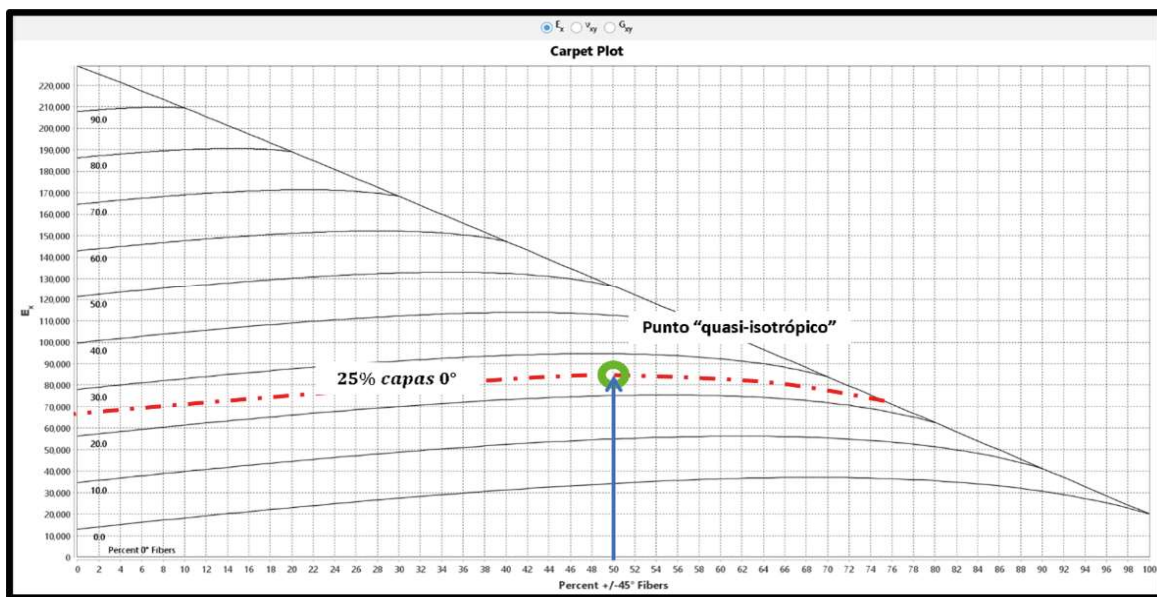


Figure 6. Localization of the “quasi-isotropic” point on the “carpet plot” diagram related to the longitudinal modulus E_x within the laminate family of the specified type $[0_m / \pm 45_n / 90_p]_s$ [Own source]

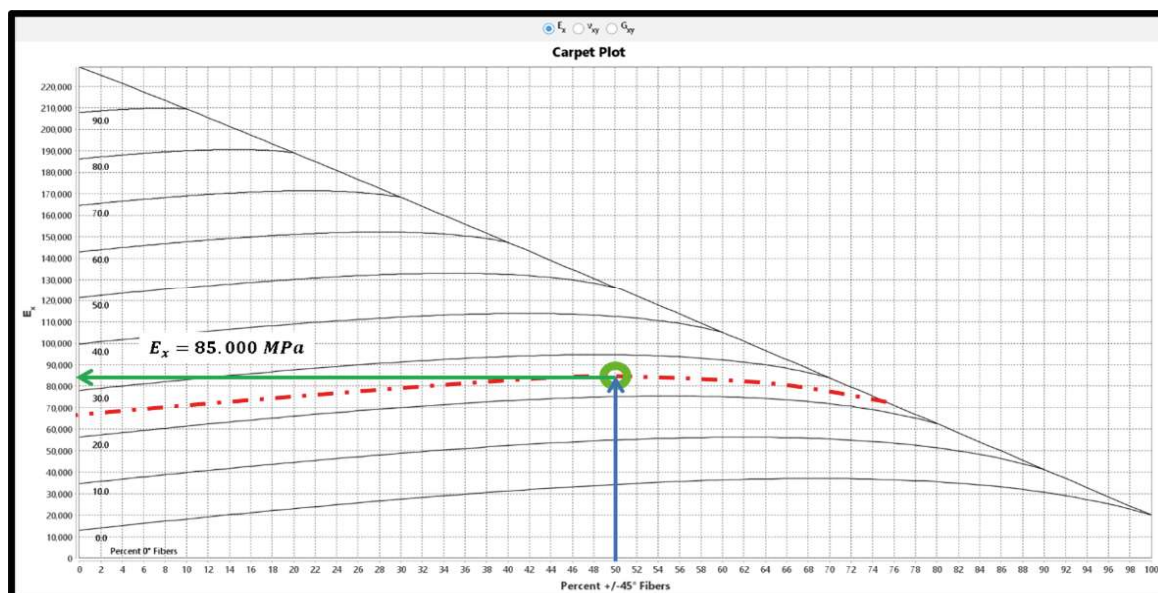


Figure 7. Longitudinal modulus estimation E_x through the “carpet plot” [Own source].

reinforcement orientations throughout the laminate layers, resulting in consistent mechanical properties in multiple directions.

Using the eLamX software, the stacking sequence is designed using the carpet-plot feature.

This feature illustrates three elastic constants: $E_{x'}$, ν_{xy} and G_{xy} on the x-axis, allowing the selection of the desired property from the options. The order axis depicts the percentage of sheets intended to have an orientation of $\pm 45^\circ$.

In order to ascertain the “quasi-isotropy” point, the laminate structure should feature an equal number of plies/sheets oriented at angles as per the following relationship:

$$\frac{180^\circ}{N+\theta^\circ} \quad \text{where } N>3 \text{ and } \theta^\circ \text{ represents the initial orientation.}$$

When $N=4$ and $\theta^\circ=0^\circ$, the relation (1) yields 45° . Thus, to reach the “quasi-isotropic” point, the orientations of the layers must be:

$$0^\circ, +45^\circ, 90^\circ \text{ and } 135^\circ (-45^\circ)$$

The stacking sequence configuration should guarantee an equal number of layers with all the specified angles. Typically, for a stacking sequence:

$$[0/45/-45/90/90/-45/45/0]_s$$

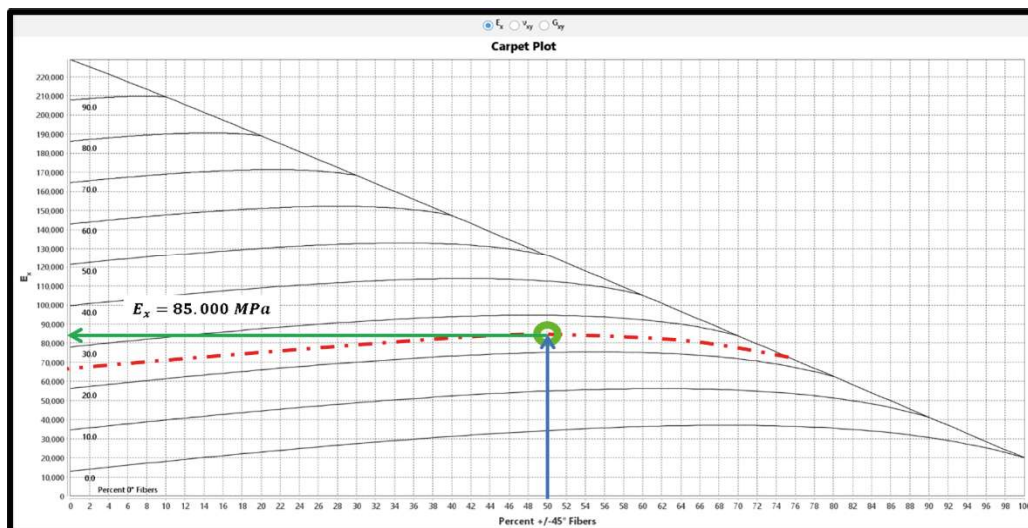


Figure 8. Estimation of shear modulus G_{xy} through the “carpet plot” [Own source].

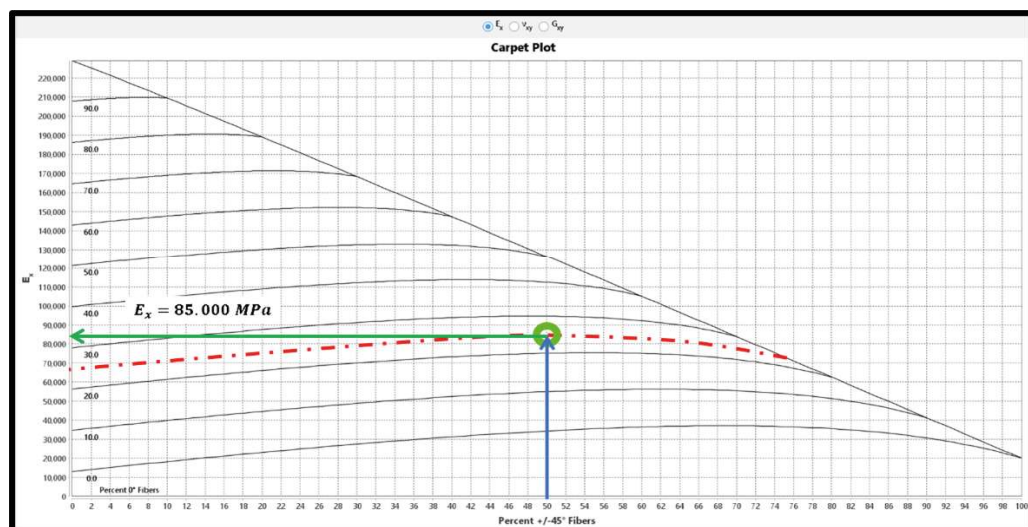


Figure 9. Estimation of Poisson's ratio ν_{xy} through the “carpet plot” [Own source].

For this laminate family, the “quasi-isotropic” point is determined by the distribution of layers as follows:

25%→0°→ 4 layers

50%→45° and 135°→ 8 layers

25%→0°→ 4 layers

With this information, “carpet-plot” is used as depicted in Figure 6 to locate the point. Under these conditions, a uniform distribution of orientations around the circumference, and designated layer percentages at specific orientations can be asserted that the laminate will demonstrate “quasi-isotropic” properties.

In (Rivas Hernández, 2023), it's noted that the variability in estimating the mechanical properties of a composite laminate between the graphic method (carpet-plot) and the classical lamination theory (CLT) is minimal, and the results obtained through this graphical methodology are deemed acceptably valid. To graphically ascertain the properties of the laminate using the “carpet plot” diagram, for instance, in the case of the longitudinal modulus E_x , a horizontal line (green line) is extended from the “quasi-isotropic” point until it intersects the ordinate axis, as illustrated in Figure 7.

The procedure is replicated to determine the shear modulus G_{xy} and Poisson's ratio ν_{xy} , following analogous steps illustrated in Figures 8 and 9, respectively.

Since the objective was to attain a material with “quasi-isotropic” properties, the longitudinal modulus is identical to the transverse modulus, denoted as $E_x=E_y$. Consequently, Poisson's ratios are also equal, $\nu_{xy}=\nu_{yx}$. Thus, the mechanical properties of a laminated composite material XC 130

300g were estimated graphically. Table 4 presents the results obtained and the comparison with those obtained through Classical Lamination Theory (CLT).

Results

Closure mechanism: As stated from the outset, the present work exclusively focuses on the design and preliminary validation of the forearm prosthetic structure, excluding from its scope the detailed engineering of the hand mechanism and the socket coupling. These components, although critical for the final functionality of the prosthesis, were considered out of reach for this initial phase and are intended to be developed in future work.

Recognizing the need for mechanical simplicity and agility during CrossFit activities, a barrel cam mechanism was proposed for the closure of the hand. This solution, illustrated in Figure 10, allows for the manual activation of a grasping motion by means of a simple rotational movement, minimizing energy expenditure and complexity.

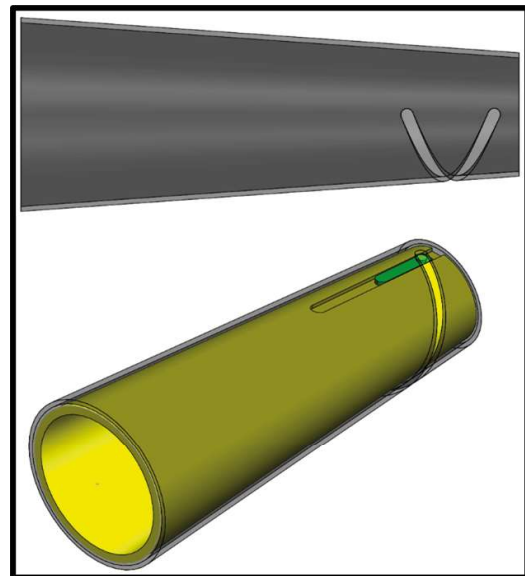


Figure 10. Slotted barrel and assembly coupling [Own source].

Table 4. Comparison of the laminate property estimations between “carpet plot” and CLT. [Own with

Carpert plot			CLT		
$E_x=$	85.000	MPa	$E_x=$	85.010,10	MPa
$G_{xy}=$	32.000	MPa	$G_{xy}=$	32.225,60	MPa
$\nu_{xy}=$	0,32		$\nu_{xy}=$	0,319	

Hand development:

One of the critical factors that greatly influences the functionality of the prosthesis, and inevitably its cost, is the engineering and robotics involved in an electronically actuated hand. The comprehensive design of a hand and its systems can serve as a dedicated topic for a bachelor's or master's thesis. However, for the scope of this initial stage, the hand design was limited to adjusting the physical characteristics of the patient's right hand without developing a full kinematic or actuation system. Figure 11 shows the simplified hand design model. This adjustment encompassed the height, width, and thickness of the palm on one hand, and the dimensions of the fingers on the other, as depicted in Figure 11.

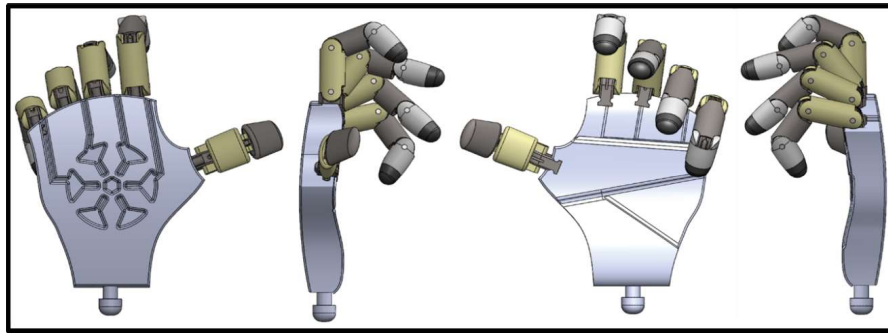


Figure 11. Left hand design [Own source].

Mechanical Female Left Arm Low-Elbow Prosthesis for CrossFit Training:

The main components of a mechanical prosthesis have been designed, which will allow for high-intensity activity without sacrificing the characteristic dynamism of CrossFit training. Currently, there is no all-encompassing solution like the one proposed that enables this sports practice (Figure 12). From here, the designs of the remaining subsystems of hand and wrist can be finalized, paying special attention to the socket, as it is the element that integrates the prosthesis with the user and plays a crucial role in its optimal functioning.

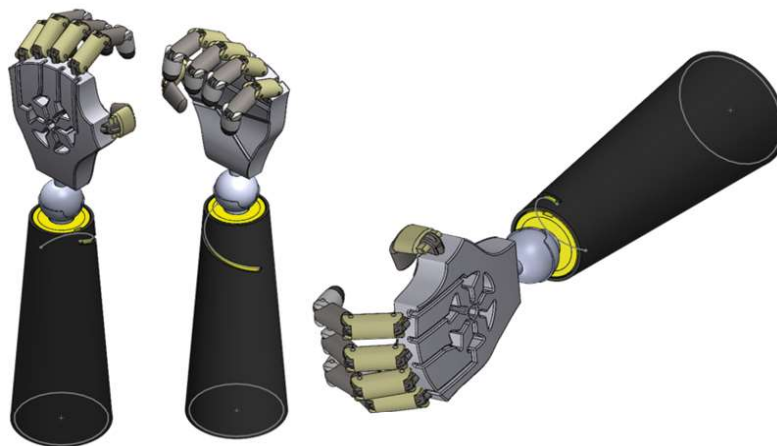


Figure 12. Mechanical Female Left Arm Low-Elbow Prosthesis [Own source].

Validation process: SolidWorks stands out as a robust digital tool for mechanical design and product validation. However, its capability to simulate composite materials is limited in the academic version. Notably, SolidWorks lacks composite materials in its material library. Consequently, to simulate components designed with composites, custom creation of materials is necessary. The data presented in Table 3 illustrates the properties estimated through the Chamis micromechanical model. Utilizing this information, the material "XC130 300g UD Prepreg Carbon fiber" is generated within the SolidWorks material library.

Table 5. Evaluation of the maximum normal stress failure criterion (Rankine criterion) in tension.

RANKINE CRITERION						
$S_x =$	2,92	MPa	<	$Y_t =$	46	MPa
$S_y =$	1,06	MPa				
$S_z =$	13,81	MPa		$X_t =$	1.500	MPa
$\tau_{xy} =$	0,26	MPa	<	SC=	46	MPa
$\tau_{xz} =$	0,26	MPa				MPa
$\tau_{yz} =$	0,2352	MPa				MPa

To streamline the configurations of various load modes for simulation, the focus was directed towards the closure mechanism, given its pivotal role within the prosthesis. For this project, 8 layers were symmetrically stacked (totaling 16 layers), all composed of the same material. Each layer has a thickness of 0.3 mm (cured), with a reference angle set at 0° degrees.

Static tension analysis: This test evaluates the behavior of the component during a “pull-up.” Figure 13 illustrates the plotting of the maximum normal stresses and the maximum shear stresses generated by a tensile force of 440 N.

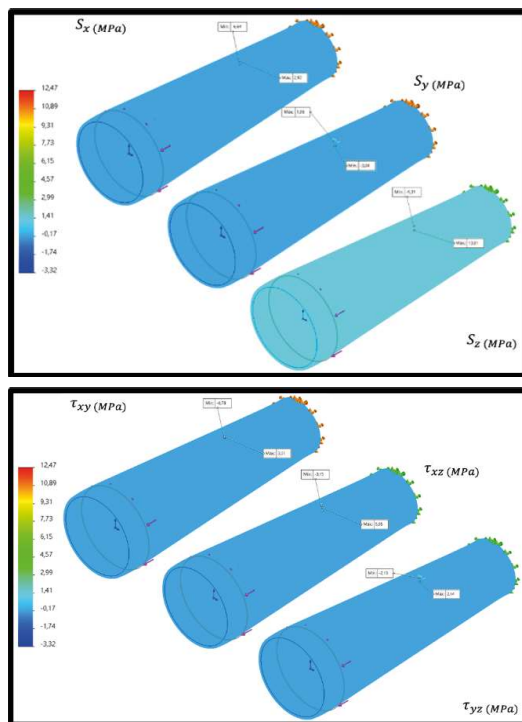


Figure 13. a) Plot of Maximum Tension Stresses $S_x=2,92$ MPa, $S_y=1,06$ MPa and $S_z=13,81$ MPa across all layers. b) Plot of Maximum Shear Stresses $\tau_{xy}=3,01$ MPa, $\tau_{xz}=5,95$ MPa and $\tau_{yx}=2,14$ MPa MPa across all layers [Own source].

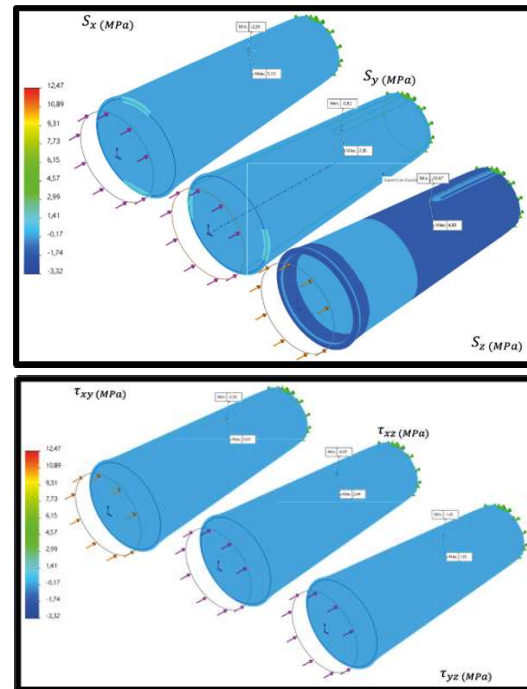


Figure 14. a) Plot of Maximum Tension Stresses $S_x=5,13$ MPa, $S_y=2,35$ MPa and $S_z=4,83$ MPa across all layers. b) Plot of Maximum Shear Stresses $\tau_{xy}=2,33$ MPa, $\tau_{xz}=4,59$ MPa and $\tau_{yx}=1,65$ MPa MPa across all layers [Own source].

Based on the comparison of the tensile simulation results (left side of the table) with the strength properties of our material (right side), it can be confirmed that the component will not fail due to the working stress level (Castro Sánchez, 2018). Additionally, obtaining the safety factor distribution yields a FS=25.56 for the worst case across all layers. Consequently, it can be concluded that the component will work properly under these loading conditions.

Static compression analysis: This test assesses the behavior of the component during a handstand or a push-up. Figure 14 displays the plot of maximum normal stresses and the maximum shear stresses generated by a compression force of 340 N.

Table 6. Evaluation of the maximum normal stress failure criterion (Rankine criterion) in compression.

CRITERIO DE FALLO DE TENSIÓN NORMAL MÁXIMA						
$S_x =$	5,13	MPa	<	$Y_c =$	86	MPa
$S_y =$	2,35	MPa				
$S_z =$	4,88	MPa	<	$X_c =$	900	MPa
$\tau_{xy} =$	2,33	MPa	<	SC=	46	MPa
$\tau_{xz} =$	4,59	MPa				MPa
$\tau_{yz} =$	1,65	MPa				MPa

Similarly, comparing the compression simulation results (left side of the table) with the strength properties of our material (right side), it can be confirmed that the component will not fail due to the working stress level. Furthermore, the safety factor distribution yields an FS=36.17 for the worst case across all layers. Therefore, it can be concluded that the component will not fail under these loading conditions (Castro Sánchez, 2018).

Discussion of simplifications and limitations:

- Dynamic effects during exercises were neglected, focusing only on static equivalent loads.
- Socket coupling and its mechanical integration were not analyzed.
- Possible stress concentrations near attachment points were not investigated in depth.

Additionally, the very high factors of safety obtained (>25) suggest that the structure is over-dimensioned for static loads. Future optimization work should aim to reduce material usage while ensuring safety under dynamic real-world conditions.

Conclusions

The design and development of a prosthetic device of this nature necessitates a collaborative effort involving various stakeholders. Active participation from patients, medical professionals, and orthopedists is paramount for accurately translating needs and capabilities into engineering design.

The proposed mechanism, while simple and familiar, offers the patient not only the ability to train but also to engage in the same activities as with her cosmetic and myoelectric prostheses. The practicality of achieving hand activation with a half-turn is emphasized, contributing to the versatility and usability of the prosthetic device. However, further work is required before manufacturing.

eLamX emerges as a valuable open-source software, greatly facilitating micromechanical analysis and the estimation of elastic and strength properties for composite material layers and laminates. Its use is underscored as a powerful tool for streamlining calculations and expediting product development processes.

While SolidWorks is a widely used and versatile tool for product design and conception, it encounters challenges in modeling textiles or non-rigid components. The limitations in modeling such components are highlighted, suggesting potential difficulties and delays in the product development process when dealing with these materials.

This project made significant simplifications to study the component's behavior. However, it's noted that SolidWorks' scope and simulation capabilities for composite materials are highly limited due to its inability to accommodate biaxial material sheets and limited capabilities for modeling complex orientations or structures. Challenges such as dealing with shell elements, meshing issues, and identifying

stress areas or singularities are highlighted as complicating factors in the simulation process.

References:

The Guardian. (2017). *3D-printed prosthetic limbs: the next revolution in medicine | 3D printing | The Guardian*. <https://www.theguardian.com/technology/2017/feb/19/3d-printed-prosthetic-limbs-revolution-in-medicine>

Ali, M. I., & Anjaneyulu, J. (2018). Effect of fiber-matrix volume fraction and fiber orientation on the design of composite suspension system. *IOP Conference Series: Materials Science and Engineering*, 455(1). <https://doi.org/10.1088/1757-899X/455/1/012104>

Belter, J. T., Segil, J. L., Dollar, A. M., & Weir, R. F. (2013). Mechanical design and performance specifications of anthropomorphic prosthetic hands: A review. *Journal of Rehabilitation Research and Development*, 50(5), 599–618. <https://doi.org/10.1682/JRRD.2011.10.0188>

Castro Sánchez, A. (2018). *Modelización micromecánica de materiales compuestos: comparativa entre modelos analíticos y numéricos (MEF)* [Trabajo de Fin de Grado]. Universidad de Sevilla.

Cordella, F., Ciano, A. L., Sacchetti, R., Davalli, A., Cutti, A. G., Guglielmelli, E., & Zollo, L. (2016). Literature review on needs of upper limb prosthesis users. In *Frontiers in Neuroscience* (Vol. 10, Issue MAY). Frontiers Media S.A. <https://doi.org/10.3389/fnins.2016.00209>

Dohin, J., Coiffier-Leone, C., Payre, P., Bayle, B., Dohin, B., & Gautheron, V. (2016). Evaluation of a multidisciplinary consultation for children's upper limb amputation. *Annals of Physical and Rehabilitation Medicine*, 59, e14. <https://doi.org/10.1016/j.rehab.2016.07.033>

Dolk, H., Loane, M., & Garne, E. (2010). The prevalence of congenital anomalies in Europe. *Advances in Experimental Medicine and Biology*, 686, 349–364. https://doi.org/10.1007/978-90-481-9485-8_20

Ibiza Granados, C. (2015). *Análisis lineal de la estabilidad de láminas de material compuesto mediante el M.E.F* [Trabajo de Fin de Grado]. Universidad de Sevilla.

Orthotic & Prosthetic Centers. (2023). *Eco-Friendly Prosthetics: The Rise of Sustainable and Biodegradable Materials | OP Centers*. <https://opcenters.com/eco-friendly-prosthetics-the-rise-of-sustainable-and-biodegradable-materials/>

Rivas Hernández, E. I. (2023). *Diseño de una prótesis mecánica de brazo izquierdo (low-elbow) femenino para entrenamientos de Crossfit* [Trabajo de Fin de Máster, Univesitat Politècnica de Catalunya]. <http://hdl.handle.net/2117/395771>

Valero, E. G. (2023, June 23). *Prótesis que mejoran la vida de los pacientes amputados*. Asociación Nacional de Amputados de España. <https://andade.es/articulos-andade/item/protesis-que-mejoran-la-vida-de-los-pacientes-amputados>

World Health Organization. (2017). Prosthetics for Orthotics: Standards & Implementation Guide Part 2. *WHO Standards for Prosthetics and Orthotics*, 22(September 2015), 1–22.

Source of Funding

This work has not received any funding.

Author's contribution:

Conceptualization: E.R.; Methodology: E.R. and O.F.; Formal Analyi: E.R. and O.F.; Writing (original draft): E.R.; Writing (review and editing): E.R. and O.F.; Supervision: O.F.

proyector 56

An industrial design journal